

Estimating 3D GRF Using a Minimal Sensor Setup: Exploiting the Concept of VPP

1st Alessandro Castellaz

Biomedical signals and systems
University of Twente
Enschede, Netherlands
a.castellaz@utwente.nl

2nd Frank J. Wouda

Biomedical signals and systems
University of Twente
Enschede, Netherlands
f.j.wouda@utwente.nl

3rd Bert-Jan F. van Beijnum

Biomedical signals and systems
University of Twente
Enschede, Netherlands
b.j.f.vanbeijnum@utwente.nl

Abstract—This paper introduces a novel method for the estimation of 3D Ground Reaction Forces (GRF) using a minimal sensing setup, aiming to overcome the limitations associated with conventional subject-specific approaches. Specifically developed for activities where the Center of Mass (CoM) closely aligns with the pelvis position, such as without bending of the torso segment, the proposed approach includes seven Inertial Measurement Units (IMUs), Pressure Insoles (PIs), and a biomechanical constraint based on the Virtual Pivot Point (VPP) concept. The method's performance was evaluated using data from eight healthy individuals engaged in various movements, including walking, jumping, landing, and lunging. Results demonstrate good accuracy in estimating anteroposterior (AP) and vertical (V) components of GRF. Some limitations were found in the mediolateral (ML) component, especially during jumping and fast walking (FW), highlighting the need for improved filtering techniques to enhance the accuracy of the total GRF estimation. This study serves as a proof of concept, with future work aimed at refining accuracy, minimizing the set of IMUs employed, and exploring applications for Activities of Daily Living (ADL) among patients affected by Osteoarthritis (OA). The proposed approach presents a promising direction in biomechanical research intending to develop a more practical system for clinical settings.

Index Terms—Ground reaction forces, inertial measurement units, pressure insoles, virtual pivot point, osteoarthritis.

I. INTRODUCTION

Insight into the loading of body joints is important for understanding disease progression, like Osteoarthritis (OA) [1]. To perform inverse dynamics analysis, Ground Reaction Forces (GRF) in combination with body kinematics are required. While body kinematics can be determined in an ambulatory manner [2], the acquisition of 3D GRF typically relies on Force Plates (FP), which are confined to laboratory settings [3], [4].

Consequently, there is a rising interest in estimating GRF outside the laboratory, and Inertial Measurement Units (IMUs) offer a viable way to do so. Karatsidis et al. used a full-body inertial motion capture system to estimate total GRF [5]. However, they employed a large set of 17 IMUs. Other studies [6], [7], combine the use of a minimal set of IMUs with machine learning techniques to estimate GRF for different activities. Although the outcomes are promising, the analysis is limited by the extensive data needed to train the neural network model, and these methods are specific to a single movement.

To decompose the estimated total GRF, Karatsidis et al. utilized a smooth transition assumption function [8], obtaining satisfactory results. However, this method is subject-specific and requires a significant amount of data to model smooth transition functions across different movements accurately. In contrast, Fluit et al. proposed a foot contact model that is versatile across movements but remains subject-specific and susceptible to individual variations due to a simplified foot-ground contact assumption [9]. Although Skals et al. made modifications to enhance accuracy, the model retains the same limitations as its predecessors [10].

The challenge of distributing forces between the feet in the double-support (DS) phase remains a critical aspect of biomechanics. Innovative solutions are required to address this problem. One such solution is utilizing the Virtual Pivot Point (VPP) [11]–[13]. The VPP represents the point where the GRF approximately intersects above the Center of Mass (CoM) during motion. Wagner et al. extend the concept of VPP beyond walking movement [11], [12], applying it to more static movements like inline lunges and squats [13].

Assuming the rigid pelvis as the CoM [14], and considering movements that do not include bending of the torso segment, Newton's equations of motion can be employed to estimate the GRF acting on the whole body [15]. This study, serving as a proof of concept, utilizes data from the proprietary sensor fusion algorithm [2] with full-body motion capture (seven sensors) but focuses on data from three segments (pelvis and feet).

In light of these considerations, our research underscores the necessity for a non-subject-specific method that can be universally applied across different movements. Therefore, we present a novel approach to estimate 3D GRF at each foot using a minimal sensor setup. This method utilizes seven IMUs, pressure insoles (PIs), and a biomechanical constraint based on the VPP concept. Moreover, the proposed approach extends its applicability beyond subject-specific considerations, demonstrating generalization across individuals.

The following sections presented in the paper illustrate the methodologies employed, followed by the main outcomes, and conclude with a discussion of limitations and perspectives for future work.

II. METHODS

This section reports the main methods used to estimate 3D components of GRF with a set of seven IMUs and PIs.

A. Participants and Measurement systems

In this study, we used data from eight healthy individuals (age: 25.13 ± 2.70 years; weight: 68.90 ± 9.29 kg; height: 1.75 ± 0.07 m) obtained from the dataset provided by Wang et al. [16]. The proposed method involves two systems: one for estimating GRF using Xsens MVN Awinda (Xsens Technologies BV, Enschede, The Netherlands) and Moticon PIs (Moticon, Munich, Germany); and an optical motion capture system (6+ series, Qualisys, Gothenburg, Sweden) and a split-belt instrumented treadmill (Motek-Forcelink B.V, Culemborg, The Netherlands) as reference. For the wearable system, we employed data from a set of seven IMUs placed on the pelvis, upper legs, lower legs, and feet. The dataset included pelvis sensor-free acceleration, as well as position and orientation relative to the lab reference frame for the feet and pelvis segments [17]. To calculate the position and orientation of the feet segments, the complete kinematic chain of the lower limbs is required.

The study included four movements: walking (at speeds of 0.25, 1, and 1.5 m/s), jumping, landing, and lunging. Particularly, the velocity of 0.25 m/s has been selected as it closely resembles the walking speed observed during Activities of Daily Living (ADL). Further measurements are necessary to extend the applicability of the method to ADL. Nonetheless, a primary hypothesis of this study is that the proposed approach is applicable beyond gait analysis alone.

Furthermore, it is essential to note that all analyzed movements feature an upright torso, signifying that the CoM aligns with the pelvis position. Nevertheless, in motions where the torso bends, this assumption is no longer valid, thereby rendering the method ineffective. In the following sections, different walking speeds will be regarded as Slow Walking (SW) for 0.25 m/s, Normal Walking (NW) for 1 m/s, and Fast Walking (FW) for 1.5 m/s.

B. Data processing

The initial step of analysis involved computing total GRF in the anteroposterior (AP), mediolateral (ML), and vertical (V) directions. Newton's equations of motion were applied to the CoM acceleration linked to the pelvis sensor (1).

$$\mathbf{F}_{\text{ext}} = m \cdot (\mathbf{a}_{\text{CoM}} - \mathbf{g}) \quad (1)$$

Here, \mathbf{F}_{ext} is the total external force vector, m is the mass of the participant, \mathbf{a}_{CoM} is the acceleration vector of the CoM and \mathbf{g} is the gravity vector pointing upwards. Pelvis sensor acceleration was filtered using a fourth-order Butterworth zero-phase band-pass filter with a cut-off frequency in the range of 0.1-5 Hz for the AP component, and 0.1-3 Hz for the ML component [15]. For the V component, an eighth-order Butterworth zero-phase low-pass filter with a cut-off frequency of 6 Hz was employed [5].

C. GRF splitting computation

Subsequently, the unitary vectors describing the GRF directions for each foot are determined. This involved computing the distance between the VPP and Center of Pressure (CoP) of each foot expressed in the same reference frame. While CoP is provided by PIs, the VPP position relies only on a few references in the literature for activities with DS phase [11]–[13]. Thus, we utilized data measured by FP to observe the VPP position across all movements. We plotted GRF originating from CoP in the sagittal plane, as depicted by Vielemeyer et al. [11]. For walking VPP was observed to be approximately $0.2 \cdot BH$ above the CoM, which is comparable to the outcomes reported by Vielemeyer et al. For the other movements, the VPP position was $0.15 \cdot BH$ for landing, $0.3 \cdot BH$ for jumping, and $0.6 \cdot BH$ for lunging. These findings were then added to the position of the pelvis segment in the lab reference frame to account for the VPP during the movements accurately. To generalize the method across all analyzed movements, we adopted a unified VPP value, denoted as VPP_{New} , which is $0.5 \cdot BH$. This value was observed to be applicable across all movements, as variations in VPP for walking and landing (motions with greater distance from VPP_{New}) were found to have minimal influence on the outcomes, unlike the other movements. For clarity, Fig. 1 shows an illustration of the VPP. The figure includes both the VPP positions found in the literature [11], [12] for walking (VPP_{Ref}) and the generalized VPP positions chosen for this work (VPP_{New}). Furthermore, the set of IMUs used is displayed, except for the left shank sensor, which is hidden.

We utilized data collected with PIs, each equipped with 13 capacitive sensors, to compute the CoP position in the lab frame. The PIs measure pressure distribution and provide the normalized CoP expressed within a dimensionless range from -0.5 to 0.5 to accommodate variation in PIs sizes. Therefore, we initially adjusted this data based on the subject's foot length. Since the foot segment reference frame is located in the ankle joint, the insole data was shifted by subtracting the AP distance between the ankle joint and the heel, obtained from the MVN Awinda output. The insole data was then transformed from the foot reference frame to the lab reference frame using foot segment orientation, and the CoP position was added to the foot segment position to obtain the CoP position in the lab reference frame. A system of equations was then formulated to compute the 3D GRF of each foot (2).

$$\begin{cases} F_{\text{AP}} = v_{\text{R-AP}} \cdot w_{\text{R}} + v_{\text{L-AP}} \cdot w_{\text{L}} \\ F_{\text{ML}} = v_{\text{R-ML}} \cdot w_{\text{R}} + v_{\text{L-ML}} \cdot w_{\text{L}} \\ F_{\text{V}} = v_{\text{R-V}} \cdot w_{\text{R}} + v_{\text{L-V}} \cdot w_{\text{L}} \end{cases} \quad (2)$$

Here, F_{AP} , F_{ML} , and F_{V} represent the components of total GRF, v_{R} and v_{L} represent the direction vectors for the right and left foot for each direction respectively (AP, ML, and V), and w_{R} and w_{L} are the unknowns representing the magnitude of the GRF for each foot. This system is over-determined,

III. RESULTS

In this section, we present the key outcomes of our study. As all the studied movements are symmetrical across the feet, the results reported here are relative to the right foot. Any outcomes displaying significant differences between the feet are highlighted and subsequently discussed. Fig. 2 displays an example of estimated GRF for SW. Here, higher peaks of force can be observed, especially during the SS phase of the ML component.

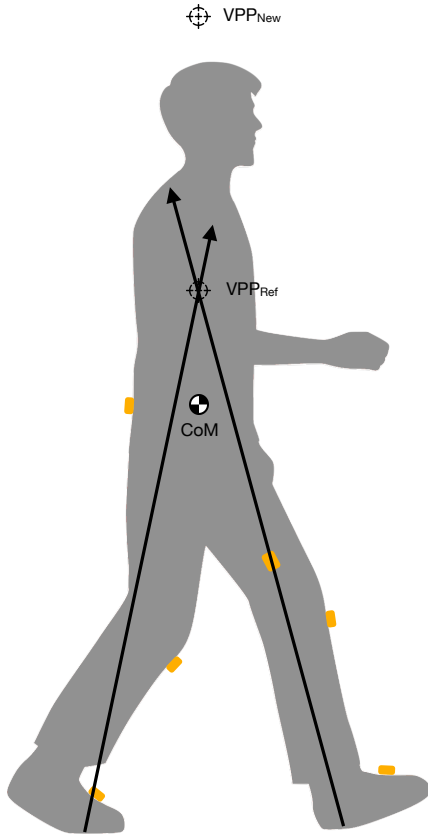


Fig. 1: VPP illustration with both literature (VPP_{Ref}) and proposed (VPP_{New}) VPP position

with two unknowns and three equations, and is solved using the least squared solution [18] for each time step. Furthermore, given that the V component of GRF must be non-negative, we constrained the solution of the system accordingly.

As a remark, the method is applied only with a DS configuration, and, when the single-stance (SS) phase is present, the total GRF is linked to the foot in contact with the ground.

D. Data analysis for results

The walking motion was divided into cycles to compare the wearable and reference systems, representing the mean and standard deviation. The V force from the force plate identified instances of contact (heel-strike and toe-off) using a 10 N threshold. The GRF was normalized to Body Weight (BW), and time was normalized as a percentage (0–100%) of the stance phase.

To estimate accuracy, Pearson's correlation coefficient (ρ) and root mean squared error (RMSE) in the percentage of BW were employed. Regarding (ρ), the correlation is defined as negligible if $0 \leq \rho \leq 0.3$, weak if $0.3 \leq \rho \leq 0.5$, moderate if $0.5 \leq \rho \leq 0.8$ and strong if $\rho \geq 0.8$ [19].

For reporting the results, the entire signal was considered, and mean and standard deviation were computed across subjects for both RMSE and ρ focusing only on the DS phase.

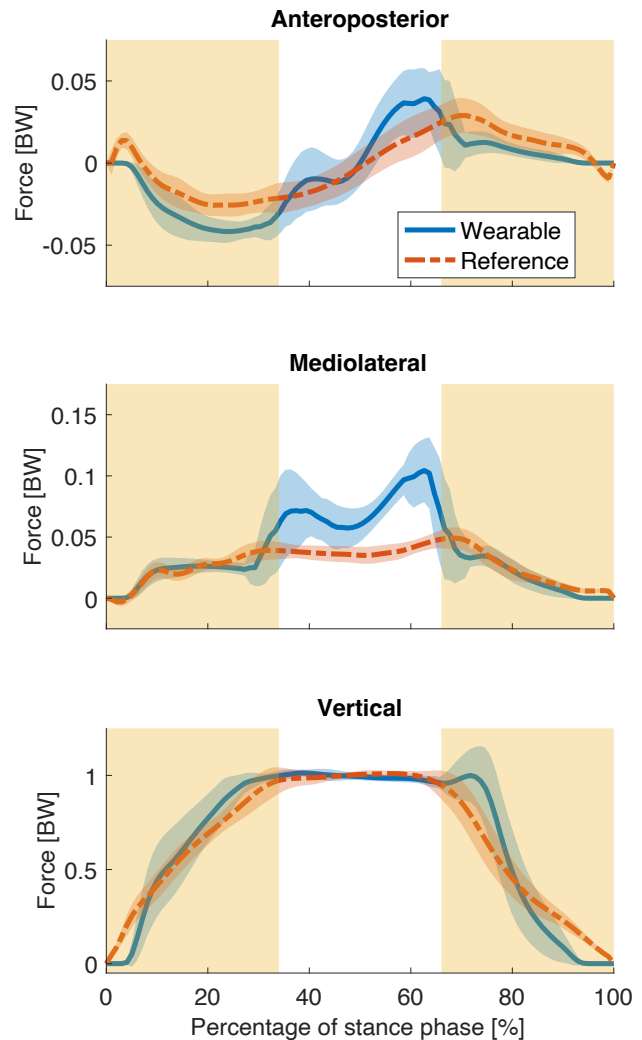


Fig. 2: GRF estimation of SW for subject 4. The solid and shaded blue curves illustrate the outcomes of the wearable system, while the solid and shaded orange curves represent the reference system. Additionally, the yellow shaded areas indicate the DS phases throughout the motion.

Subsequently, Fig. 3 displays an example of the estimated GRF for a lunging movement. Also here, peaks of forces can be noticed throughout the signal, again mainly in the SS of the ML component. In Table I complete findings for this study are

presented. Here, only the DS phase is considered, and, mean and standard deviation were computed across the subjects.

IV. DISCUSSION

To the best of our knowledge, the proposed method is the first that generalizes the estimation of 3D GRF for a diverse set of movements using a minimal set of IMUs. While the dataset for this study comprises only 8 subjects, the findings exhibit promising outcomes across various individuals, thus indicating the non-subject-specific nature of the proposed method.

The shear components of GRF are usually challenging to accurately estimate, primarily due to their smaller magnitudes. However, for the AP component, the method displays good accuracy. Indeed, strong correlation and low RMSE, lower than $9.18 \pm 1.84\%$ of BW, were observed for all movements analyzed except for jumping. For this activity, the estimates are less accurate, primarily attributed to the frequency used to filter pelvis sensor acceleration. For this reason, the cut-off frequency should be adjusted to accommodate movements characterized by rapid changes in acceleration.

Concerning the ML component, it is clear that the outcomes are less accurate, especially during lunge and FW. As mentioned earlier, this is primarily due to the filtering of pelvis sensor acceleration. Additionally, the signal-to-noise ratio is lower for this component, negatively influencing the method. As illustrated in Fig. 3, higher peaks of force can be observed, particularly in the SS phase. However, for some subjects, these peaks were observed throughout the entire contact phase in all three directions leading to larger errors and negative correlation coefficients. This phenomenon may be explained by the fact that data collection was performed on a belted treadmill, potentially introducing errors in IMU measurements due to mechanical vibrations, motion, and additional accelerations that the sensors might interpret as body motion. Thus, proper filtering techniques have to be applied to address these issues effectively. Anyway, the ML component of force during SW, as depicted by Fig. 2, accurately represents the DS phase compared to the SS phase.

Regarding the V component, it shows accurate results with a strong correlation. Nonetheless, the RMSE is approximately 29% of the BW. Pelvis acceleration filtering is crucial also in this context, as the total GRF derived from the pelvis sensor, compared to FP measurements, exhibited an RMSE around 20% of the BW, with higher peaks observed during FW and jumping. As a last remark, some differences were found between feet. As shown in Table I, bold outcomes report significant differences (larger than 0.1) in Pearson's correlation. Again, this difference is notable for movements like FW or jumping, especially in the ML component. Thus, further research is essential to refine the accuracy of total GRF estimation, thereby improving the overall accuracy of the proposed method.

As a remark, the metrics used in the results for RMSE are expressed as % BW. Since the results for shear components are lower than the V component, relative metrics could be considered. However, in the literature, the results are reported with

the % BW metrics indiscriminately for all three components [5].

The method's performance in estimating GRF during walking closely aligns with previous studies that used more extensive sensor setups, such as Karatsidis et al. [5]. However, the proposed approach aims to achieve similar accuracy with a minimal set of seven IMUs and PIs, making the method more practical for clinical applications. In terms of the AP and V components, our results closely resemble the observations made by Karatsidis et al., showing only marginal differences in the case of the V component. Specifically, during the initial DS phase, averaging outcomes from SW, NW, and FW, they achieved strong correlations of 0.918 and 0.946, and a RMSE of 5.8 ± 2.3 and $14.3 \pm 7.7\%$ of BW for AP and V components, respectively. Regarding the ML component, they demonstrated better outcomes with a correlation coefficient of 0.79. Nevertheless, the RMSE was comparable to our findings, standing at 3.0% of BW.

Furthermore, when comparing the outcomes of our study to those of Wouda et al. [6], who specifically focused on the V component of GRF during running, our method demonstrates comparable performance. Wouda et al. achieved a RMSE of less than 27% of BW, with our RMSE being less than 28.71%. However, it is important to note that this study concentrates only on running, an activity that lacks the DS phase, the main focus of our investigation.

This comparison highlights the method's potential to achieve accuracy similar to more complex sensor configurations and machine learning techniques, emphasizing its practicality for OA patients.

A. Limitations

The proposed method for predicting 3D GRF with a minimum sensing setup shows promising results but faces some challenges. Soft tissue artifacts [20] in IMUs can introduce inaccuracies, especially during activities like jumping and FW where rapid changes in acceleration occur more frequently. Calibration and standardization of PIs are necessary to overcome inaccuracies in estimating the CoP, particularly considering variations in footwear, insole placement, and individual foot anatomy [21].

Additionally, relying on a single IMU for calculating total GRF restricts the range of movements that may be studied. This is because the assumption that the rigid pelvis embodies the CoM is no longer valid during motions involving the bending of the torso. Proper consideration and refinement of these aspects are crucial for the method to be successfully applicable in different biomechanical scenarios and clinical settings.

As a final remark, conducting a more comprehensive investigation with an extended dataset could further validate the proposed approach and enhance its robustness.

B. Future Perspectives

This study, serving as a proof of concept, utilizes data obtained from Xsens Awinda output, employing a set of seven

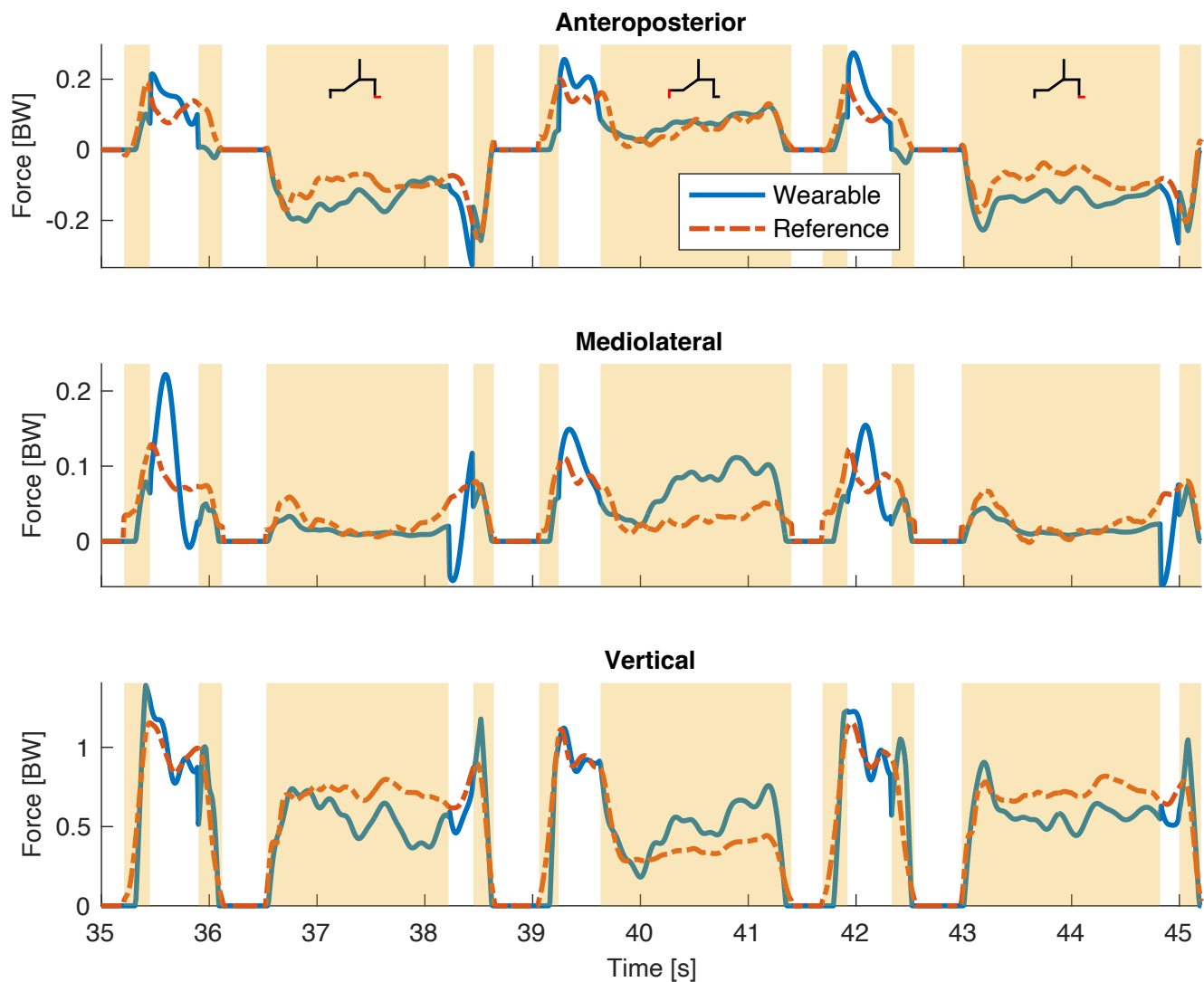


Fig. 3: GRF Estimation of Lunging for Subject 4: A 10-second snapshot overview. The solid blue curve depicts the outcomes of the wearable system, while the solid orange curve represents the reference system. Yellow shaded areas denote the DS phases during the motion. The top section of the figure displays the states of the lunging motion, with the right foot highlighted in red.

IMUs. Building upon the work of Refai et al. [15], our objective is to extend this method using a minimized set of three IMUs (pelvis and feet) through the implementation of an Extended Kalman Filter (EKF). Minimization of IMUs utilized is critical to achieve the least invasive system possible for OA patients. Furthermore, an intriguing research direction would involve ADL in the analysis, as they are of crucial importance in the everyday lives of OA patients.

Additionally, here the VPP is considered as a constant quantity above the CoM position. However, Wagner et al. [13] proposed a constant VPP of $0.9 \cdot BH$ which is placed slightly under VPP_{New} . Therefore, future work could be conducted to optimize the position of the VPP for the presented approach.

Another possible next step would be a more in-depth examination of the VPP position. First, an interesting investigation topic may be the link between VPP and a certain quantity measured with inertial sensors. Moreover, it is possible to include AP and ML position components to fine-tune the method's accuracy, especially for movements like forward jumping or variable walking speeds. Finally, to enhance accuracy, a hybrid model might be built by integrating machine learning techniques and VPP constraints to create a physics-informed Neural Network (NN) model. Additionally, augmenting the dataset with synthetic data generated from actual datasets can significantly improve model training efficiency.

TABLE I: Correlation and RMSE for estimated GRF for right and left (in brackets) foot. Significant differences between the feet are highlighted in bold.

	ρ_{AP} (mean \pm std)	ρ_{ML} (mean \pm std)	ρ_V (mean \pm std)	RMSE _{AP} (mean \pm std) %BW	RMSE _{ML} (mean \pm std) %BW	RMSE _V (mean \pm std) %BW
SW	0.85 \pm 0.13 (0.86 \pm 0.05)	0.62 \pm 0.18 (0.68 \pm 0.19)	0.94 \pm 0.03 (0.93 \pm 0.04)	1.28 \pm 0.27 (1.42 \pm 0.49)	1.39 \pm 0.28 (1.44 \pm 0.46)	17.00 \pm 2.47 (17.13 \pm 2.23)
NW	0.91 \pm 0.03 (0.90 \pm 0.05)	0.39 \pm 0.25 (0.54 \pm 0.16)	0.88 \pm 0.04 (0.88 \pm 0.04)	5.58 \pm 1.02 (5.11 \pm 0.78)	3.01 \pm 0.65 (2.75 \pm 0.62)	25.27 \pm 3.27 (24.57 \pm 2.11)
FW	0.91 \pm 0.04 (0.91 \pm 0.05)	0.14 \pm 0.40 (0.39 \pm 0.27)	0.85 \pm 0.09 (0.86 \pm 0.06)	9.18 \pm 1.84 (8.10 \pm 1.57)	4.31 \pm 1.37 (3.76 \pm 1.11)	28.71 \pm 7.24 (26.91 \pm 5.41)
Jump	0.24 \pm 0.13 (0.14 \pm 0.14)	0.61 \pm 0.19 (0.34 \pm 0.20)	0.76 \pm 0.13 (0.48 \pm 0.23)	6.53 \pm 1.56 (5.46 \pm 1.51)	3.99 \pm 1.27 (4.36 \pm 1.23)	26.88 \pm 10.82 (25.59 \pm 9.67)
Land	0.86 \pm 0.09 (0.76 \pm 0.19)	0.73 \pm 0.11 (0.78 \pm 0.11)	0.86 \pm 0.08 (0.88 \pm 0.04)	2.67 \pm 0.56 (3.57 \pm 1.76)	3.19 \pm 0.77 (3.74 \pm 0.92)	20.35 \pm 3.56 (21.58 \pm 3.64)
Lunge	0.89 \pm 0.03 (0.89 \pm 0.04)	0.13 \pm 0.28 (0.09 \pm 0.29)	0.80 \pm 0.07 (0.81 \pm 0.07)	5.28 \pm 1.13 (5.52 \pm 1.27)	3.72 \pm 1.23 (3.83 \pm 1.11)	17.56 \pm 4.36 (17.98 \pm 4.92)

V. CONCLUSION

In this study, we introduced an innovative approach for the estimation of 3D GRF with minimal sensing across different activities, eliminating the subject specificity constraint of traditional methods. While further research is required to refine the accuracy of total GRF estimation, our preliminary findings indicate promising outcomes, potentially expanding the estimation of GRF.

ACKNOWLEDGMENTS

We extend our appreciation to Junhao Zhang for his valuable contributions to the review process and Huawei Wang for providing the dataset essential to this study.

REFERENCES

- [1] Johanne Martel-Pelletier, Andrew J. Barr, Flavia M. Cicuttini, Philip G. Conaghan, Cyrus Cooper, Mary B. Goldring, Steven R. Goldring, Graeme Jones, Andrew J. Teichtahl, and Jean-Pierre Pelletier. Carbamate-modified cross-linked dextran microparticles suppress the progression of osteoarthritis by ROS scavenging. *Biomaterials Science*, 9(18):6357–6368, 2021.
- [2] Daniel Roetenberg, Henk Luinge, and Per Slycke. Xsens mvn: Full 6dof human motion tracking using miniature inertial sensors. *Xsens Technologies*, 2009.
- [3] Erfan Shahabpoor and Aleksandar Pavic. Measurement of walking ground reactions in real-life environments: A systematic review of techniques and technologies. *Sensors*, 17(9):2085, 2017.
- [4] P. H. Veltink, C. B. Liedtke, E. Droog, and H. van der Kooij. Measurement in sports biomechanics. In *Proceedings of Measuring Behavior 2005: 5th International Conference on Methods and Techniques in Behavioral Research*, pages 646–648, 2005.
- [5] Angelos Karatsidis, Giovanni Bellusci, H. Martin Schepers, Mark De Zee, Michael S. Andersen, and Peter H. Veltink. Estimation of ground reaction forces and moments during gait using only inertial motion capture. *Sensors*, 17(1):75, 2017.
- [6] Frank J Wouda, Matteo Giuberti, Giovanni Bellusci, Erik Maartens, Jasper Reenalda, Bert-Jan F van Beijnum, and Peter H Veltink. Estimation of vertical ground reaction forces and sagittal knee kinematics during running using three inertial sensors. *Sensors*, 15(12):28365–28382, 2015.
- [7] Serena Cerfoglio, Manuela Galli, Marco Tarabini, Filippo Bertozzi, Chiarella Sforza, and Matteo Zago. Machine learning-based estimation of ground reaction forces and knee joint kinetics from inertial sensors while performing a vertical drop jump. *Sensors*, 21(22):7709, 2021.
- [8] Lei Ren, Richard K. Jones, and David Howard. Whole body inverse dynamics over a complete gait cycle based only on measured kinematics. *Journal of Biomechanics*, 41(12):2750–2759, 2008.
- [9] René Fluit, M.S. Andersen, S. Kolk, Nicolaas Jacobus Joseph Verdonchot, and Hubertus F.J.M. Koopman. Prediction of ground reaction forces and moments during various activities of daily living. *Journal of Biomechanics*, 47(10):2321–2329, 2014.
- [10] Sebastian Skals, Moon Ki Jung, Michael Damsgaard, and Michael Skipper Andersen. Prediction of ground reaction forces and moments during sports-related movements. *Multibody System Dynamics*, 39(3), March 2017.
- [11] Johanna Vielemeyer, Lucas Schreff, Stefan Hochstein, and Roy Müller. Virtual pivot point: Always experimentally observed in human walking? *PLoS ONE*, 18(10):e0292874, 2023.
- [12] Lucas Schreff, Daniel F.B. Haeufle, Alexander Badri-Spröwitz, Johanna Vielemeyer, and Roy Müller. Virtual pivot point in human walking: Always experimentally observed but simulations suggest it may not be necessary for stability. *PLoS ONE*, 18(10):e0292874, 2023.
- [13] Heiko Wagner, Oliver Schmitz, and Kim J. Boström. The virtual pivot point concept improves predictions of ground reaction forces. *Frontiers in Bioengineering and Biotechnology*, 12, 2024.
- [14] Marianne J Floor-Westerdijk, H Martin Schepers, Peter H Veltink, Edwin H F van Asseldonk, and Jaap H Buurke. Use of inertial sensors for ambulatory assessment of center-of-mass displacements during walking. *IEEE Transactions on Biomedical Engineering*, 59(7):2080–2084, 2012.
- [15] Mohamed Irfan Mohamed Refai, Bert-Jan F van Beijnum, Jaap H Buurke, and Peter H Veltink. Portable gait lab: Estimating over-ground 3d ground reaction forces using only a pelvis imu. *Sensors*, 20:6363, 2020.
- [16] Huawei Wang, Akash Basu, Guillaume Durandau, and Massimo Sartori. Comprehensive kinetic and emg dataset of daily locomotion with 6 types of sensors, 2021.
- [17] D. Roetenberg, H.J. Luinge, C.T.M. Baten, and P.H. Veltink. Compensation of magnetic disturbances improves inertial and magnetic sensing of human body segment orientation. *IEEE Transactions on Neural Systems and Rehabilitation Engineering*, 13(3):497–500, 2005.
- [18] Guido Gerig. Least squares, pseudo-inverses, pca & svd. <http://sci.utah.edu/~gerig/CS6640-F2012/Materials/pseudoinverse-cis61009s110.pdf>, 2012. Chapter 11.
- [19] Emily S Matijevich, Lauren M Branscombe, Leon R Scott, and Karl E Zelik. Ground reaction force metrics are not strongly correlated with tibial bone load when running across speeds and slopes: Implications for science, sport and wearable tech. *PLoS ONE*, 14(1):e0210000, 2019.
- [20] Haye Kamstra, Erik Wilmes, and Frans C.T. van der Helm. Quantification of error sources with inertial measurement units in sports. *Sensors*, 22:9765, 2022.
- [21] Pauline Morin, Antoine Muller, Charles Pontonnier, and Georges Dumont. Evaluation of the foot center of pressure estimation from pressure insoles during sidestep cuts, runs and walks. *Sensors*, 22:5628, 2022.